

Properties of SiC Ceramics Sintered via Liquid Phase Using $\text{Al}_2\text{O}_3 + \text{Y}_2\text{O}_3$, $\text{Al}_2\text{O}_3 + \text{Yb}_2\text{O}_3$ and $\text{Al}_2\text{O}_3 + \text{Dy}_2\text{O}_3$ as Additives: a Comparative Study

Sebastião Ribeiro^{a*}, Giseli Cristina Ribeiro^a, Marcela Rego de Oliveira^a

^aDepartamento de Engenharia de Materiais – DEMAR, Escola de Engenharia de Lorena – EEL, Universidade de São Paulo – USP, Pólo Urbo Industrial, Gleba A16, CP 116, CEP 12608-970, Lorena, SP, Brazil

Received: July 22, 2014; Revised: May 23, 2015

Silicon carbide (SiC) ceramics show excellent performance at high temperatures. Due to the high covalence of Si-C bonds, these ceramics are produced successfully only via liquid phase sintering (LPS). In this work, SiC ceramics were sintered via LPS using eutectic mixtures of $\text{Al}_2\text{O}_3 + \text{Y}_2\text{O}_3$, which served as a standard for comparison, $\text{Al}_2\text{O}_3 + \text{Yb}_2\text{O}_3$ and $\text{Al}_2\text{O}_3 + \text{Dy}_2\text{O}_3$. The oxides mixtures were used to form liquid phase during the SiC sintering. Mixtures of SiC and additives were ground, pressed at 300 MPa and sintered at 1950 °C for 2 hours. All mixtures showed similar hardness, fracture toughness and flexural strength slightly different. Also the microstructure and crystalline phase were similar, showing that the ytterbium's and dysprosium's oxides can be also used as additive as well the most used oxide, yttrium oxide.

Keywords: silicon carbide, liquid phase sintering, rare earths oxide, mechanical properties

1. Introduction

SiC ceramics have many applications because they allow the combination of important properties such as low density, high elastic and rupture modulus, high thermal shock resistance, and high resistance to corrosion and oxidation at high temperatures¹⁻¹³.

One of the properties of SiC ceramics that limits many applications is their low fracture toughness. Research investments have been made in the control or improvement of this property using additives in liquid phase sintering, as well as in the control of morphology and grain size during sintering and post-sintering heat treatments^{9,10}.

Various additives have been studied for the formation of this liquid phase in order to improve sintering and promote the formation of favorable microstructures with higher fracture toughness values than the existing ones. Examples of well known additives are mixtures of Al_2O_3 or AlN with earth oxides (Y_2O_3 , La_2O_3 , Sm_2O_3 , Tb_2O_3)^{2-4,9,10}. Among the aforementioned rare earth oxides, the one best known for production of the liquid phase during sintering is Y_2O_3 , which appears in numerous publications¹⁻¹³. Yttrium is one of the four most abundant rare earths and dysprosium and ytterbium occupy the eighth and ninth place^{13,14}.

The most significant properties of the liquids used in liquid phase sintering are the melting temperature and the degree of wetting of these liquids in the ceramic base material, which is measured by the contact or wetting angle, θ ¹⁵⁻⁸¹. The melting temperature and wettability of the $\text{Al}_2\text{O}_3 - \text{Y}_2\text{O}_3$, $\text{Al}_2\text{O}_3 - \text{Yb}_2\text{O}_3$ and $\text{Al}_2\text{O}_3 - \text{Dy}_2\text{O}_3$ additive systems in SiC have been studied and are described in the literature^{7,15}.

This article evaluates the properties of compactability, densification, rupture modulus, fracture toughness and hardness

of SiC ceramics doped with the $\text{Al}_2\text{O}_3 + \text{Y}_2\text{O}_3$, $\text{Al}_2\text{O}_3 + \text{Yb}_2\text{O}_3$ and $\text{Al}_2\text{O}_3 + \text{Dy}_2\text{O}_3$ systems. The values of these properties of these additives will be used to select the best system for sintering SiC from the technical standpoints.

2. Experimental

In this work three mixtures were prepared: SiC + 10 vol.% ($\text{Al}_2\text{O}_3 + \text{Y}_2\text{O}_3$), SiC + 10 vol.% ($\text{Al}_2\text{O}_3 + \text{Yb}_2\text{O}_3$) and SiC + 10 vol.% ($\text{Al}_2\text{O}_3 + \text{Dy}_2\text{O}_3$). Each mixture contained 90% in volume of SiC and 10% in volume of additives.

The SiC used here was of the type GRADE BF-12 from Hermann C Starck. The characteristics of the SiC are listed in the Table 1.

The purity and average particle sizes of the oxides are listed in the Table 2.

The quantities of Al_2O_3 , Y_2O_3 , Yb_2O_3 and Dy_2O_3 were calculated based on the phase diagrams^{8,15}. Because the $\text{Al}_2\text{O}_3 + \text{Dy}_2\text{O}_3$ system lacks a phase diagram, a presumably eutectic composition was chosen as the basis, the $\text{Al}_2\text{O}_3 + \text{Yb}_2\text{O}_3$ phase diagram¹⁵. Table 3 lists the quantities of SiC, Al_2O_3 , Y_2O_3 , Yb_2O_3 and Dy_2O_3 used in each mixture.

The powders used in each mixture (ALY, ALYB and ALD) were placed in an attrition mill with isopropyl alcohol P.A. and mixed for 6 hours at 300 rpm. After mixing, the suspensions were vacuum dried at 90 °C in a rotary evaporator until they reached a constant weight.

The powders of the mixtures were desagglomerated in a 20 mesh sieve and pressed under 300 MPa in an isostatic press with the following dimensions: 52.4 mm × 29.2 mm × 6.5 mm. After pressing, the samples were measured and weighed, and the density of each mixture was calculated based on the

*e-mail: sebastiao@demar.eel.usp.br

mass to volume ratio. The relative densities were calculated based on the rule of mixtures.

Samples of each composition were sintered in a furnace at 1950 °C for two hours in an argon atmosphere, applying a heating and cooling rate of 30 °C/min.

The density of the sintered samples was also calculated by the geometrical method, but the real density was determined by helium pycnometry. The densities of SiC mixtures were calculated based on the sintered and real density values of the samples.

The sintered plate-shaped samples were ground on both sides using a grinding wheel with 120 µm grains, after which they were cut into 39 × 4 × 3 mm specimens, using a diamond disc. Some of these specimens were used to determine the bending modulus of rupture and some of them to measure the fracture toughness.

To measure the modulus of rupture, the specimens were subjected to a 3-point bending test using a standard MTS 64205A-01 Bend Fixture with 20 mm spacing between rollers. An MTS 810 universal testing machine with a 5 kN load cell was used, applying a loading rate of 10 N/second. The modulus of rupture was calculated using following equation:

$$\sigma_f = \frac{3P_f L}{2bh^2} \quad (1)$$

where σ_f is the fracture stress or modulus of rupture (MPa); P_f is the maximum load withstood by the body (N), L is the distance between the two rollers (mm), b is the width of the test specimen (mm), and h is the height of the test specimen (mm)¹¹.

The SEVNB (Single Edge V-Notched Beam) method was used to determine the fracture toughness. Groups of seven test specimens were placed on a steel plate in preparation for notching. A 0.02 mm thick razor blade and 6 µm diamond paste were used to produce the coarse notches, followed by 1 µm paste to produce fine notches. The dimensions of the radius of curvature of the notches were on average equal to 6 µm. After notching, the samples were subjected to three-point bending using the same aforementioned device and testing machine operating at a speed of 0.5 mm/min.

After the samples fractured, the notches were measured using a stereoscopic microscope with a precise graduated scale. The fracture toughness, K_{IC} , was calculated using the following equations:

$$K_{IC,SEVNB} = \frac{F}{B\sqrt{W}} \frac{S_1}{W} \frac{3\sqrt{a}}{2} Y^* \quad (2)$$

$$\alpha = \frac{a}{W} \quad (3)$$

$$Y^* = 1.964 - 2.837\alpha + 13.7714\alpha^2 - 23.250\alpha^3 + 24.129\alpha^4 \quad (4)$$

where $K_{IC,SEVNB}$ is the mode I fracture toughness (MPa.m^{1/2}) determined by the SEVNB method, F is the fracture load (MN) at the instant of rupture, B is the sample thickness, W is the height of the sample, S_1 is the distance between the two rollers, α is the ratio between notch size (depth) and height of the sample, and Y is the shape factor. The unit of B , W and S_1 is the meter^{9,11}.

For the microstructural evaluation, the samples were sanded, polished with a diamond suspension of up to 1 µm and etched with sodium tetraborate for 5 min at 770 °C, using a LEO 1450VP scanning electron microscope.

The phases in the samples of the three compositions were analyzed by X-ray diffraction using JCPDS XRD patterns. This analysis was performed using a Panalytical Model Empyrean X-ray diffractometer equipped with a copper filter.

For the hardness measurements, samples were sanded, polished and subjected to Vickers indentations using a load of 19.62 N for 15 seconds.

Table 1. Characteristics properties of the SiC powder.

Characteristic	Values
Chemical composition (%)	
Carbon (C)	30.1
Oxygen (O)	1.3
Free silicon (Si)	0.1
Impurities (%)	
Iron (Fe)	0.01
Aluminium (Al)	0.02
Calcium (Ca)	0.00
Physical characteristic	
Area superficial (m ² /g)	11.4
SiC beta (%)	95.7
D _{50%} (µm)	0.8

Table 2. Purity and average particle size (D₅₀) of the oxides.

	Al ₂ O ₃	Dy ₂ O ₃	Yb ₂ O ₃	Y ₂ O ₃
Purity (%)	99.8	99.9	99.9	99.9
D₅₀ (µm)	1.0	3.8	4.8	0.8

Table 3. Composition and respective code of each mixture under study

Mixtures	Code	Compounds/quantities (g)				
		SiC	Al ₂ O ₃	Y ₂ O ₃	Yb ₂ O ₃	Dy ₂ O ₃
SiC+10vol.%(Al ₂ O ₃ +Y ₂ O ₃)	ALY	120	11.25	6.60	0.00	0.00
SiC+10vol.%(Al ₂ O ₃ +Yb ₂ O ₃)	ALYB	120	12.76	0.00	9.39	0.00
SiC+10vol.%(Al ₂ O ₃ +Dy ₂ O ₃)	ALD	120	12.10	0.00	0.00	8.45

3. Results and Discussion

Table 4 describes some of the properties of the three mixtures under study.

The density of the sintered ALY mixture shows value close to those reported in the literature, about 97%. The literature does not have standards of comparison for the other two mixtures, because they are only recently being studied in greater depth. A comparison of the ALY, ALYB and ALD mixtures indicates that the densification of the ALD ceramics was slightly greater than the ALYB mixture, which was similar to the ALY mixture. In practice, it can be considered that the three mixtures show an identical densification behavior.

The fracture toughness of samples of the ALYB and ALD mixtures is slightly higher than the ALY mixture, but the slight difference leads us to conclude that the former are as tough as the latter.

Likewise, the result for the ALY sample is in the standards found in the literature; hence, it can be stated that the two new mixtures also show interesting and promising results.

As for the modulus of rupture, the ALYB and ALD ceramics showed much higher values than the ALY ceramic, and these values were considered very good in terms of mechanical strength, indicating a slight advantage in sintering SiC with these two new oxides.

Interestingly, the three mixtures showed very similar results in terms of the mechanical properties under study. This tendency has been demonstrated in previous studies, particularly with regard to the wetting angle, and can be justified by the similarities among the rare earths elements¹⁵.

Figure 1 shows X-ray diffraction patterns of the sintered samples for three mixtures, which presented the following phases: (ALY) α-SiC, β-SiC, Al₂O₃, Y₃Al₅O₁₂; (ALYB) α-SiC, β-SiC, Al₂O₃, Yb₃Al₅O₁₂ and (ALD) α-SiC, β-SiC, Al₂O₃, Dy₃Al₅O₁₂. The rare earth oxides form a solid solution and the formation of the RE₃Al₅O₁₂ phase showing that Dy₂O₃ and Yb₂O₃ have the same behavior as Y₂O₃¹⁰.

As the densities were similar for sintered samples (Table 4) of the three mixtures, it can be attributed to the Dy₃Al₅O₁₂ phase as responsible for the biggest modulus of rupture for ALD sample than ALYB and ALY.

Figure 2 shows micrographs of the three SiC ceramics sintered at 1950 °C for 2 hours. The micrographs on the left (a, b and c) show the ground, sanded and polished surfaces etched with sodium tetraborate for 5 min at 770 °C. These

micrographs show microstructures consisting of small grains. Also note that the microstructure of the ceramic obtained with the ALYB mixture (micrographs b and e) is slightly coarser than the other two. A comparison of these microstructures with the properties described in Table 4 leads to the conclusion that, albeit coarser, the structure of the ALYB ceramic did not show significant differences in its measured properties.

Micrographs d, e and f illustrate the fracture surfaces of the ceramics under study, showing the type of fracture and the secondary phases produced by the additives. Note that, in the three cases, the fractures are predominantly intergranular, because SiC grains do not have a very high aspect ratio, the three compositions also do not show very high fracture toughness values.

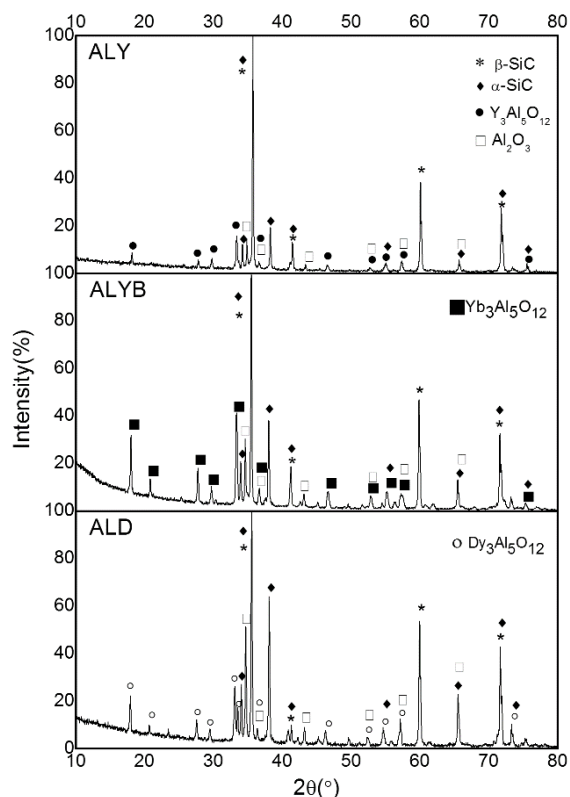


Figure 1. X-ray diffractograms patterns of sintered mixtures ALY, ALYB and ALD.

Table 4. Density, fracture toughness, modulus of rupture and hardness of the compacted and sintered samples.

Measured properties	Mixtures		
	ALY	ALYB	ALD
Green density (g/cm ³)	1.75 ± 0.01	1.82 ± 0.02	1.80 ± 0.01
Relative green density (%)	52.87 ± 0.52	53.53 ± 0.61	53.41 ± 0.48
Sintered density (g/cm ³)	3.21 ± 0.04	3.26 ± 0.02	3.24 ± 0.01
Real density (g/cm ³)	3.31 ± 0.01	3.36 ± 0.01	3.33 ± 0.01
Sintered relative density (%)	96.98	97.02	97.30
K _{IC,SEVNB} (MPa.m ^{1/2})	3.45 ± 0.20	3.51 ± 0.16	3.51 ± 0.15
Modulus of rupture (MPa)	453 ± 43	478 ± 91	501 ± 69
Vickers hardness (GPa)	23.43 ± 1.79	23.05 ± 1.25	24.75 ± 1.63

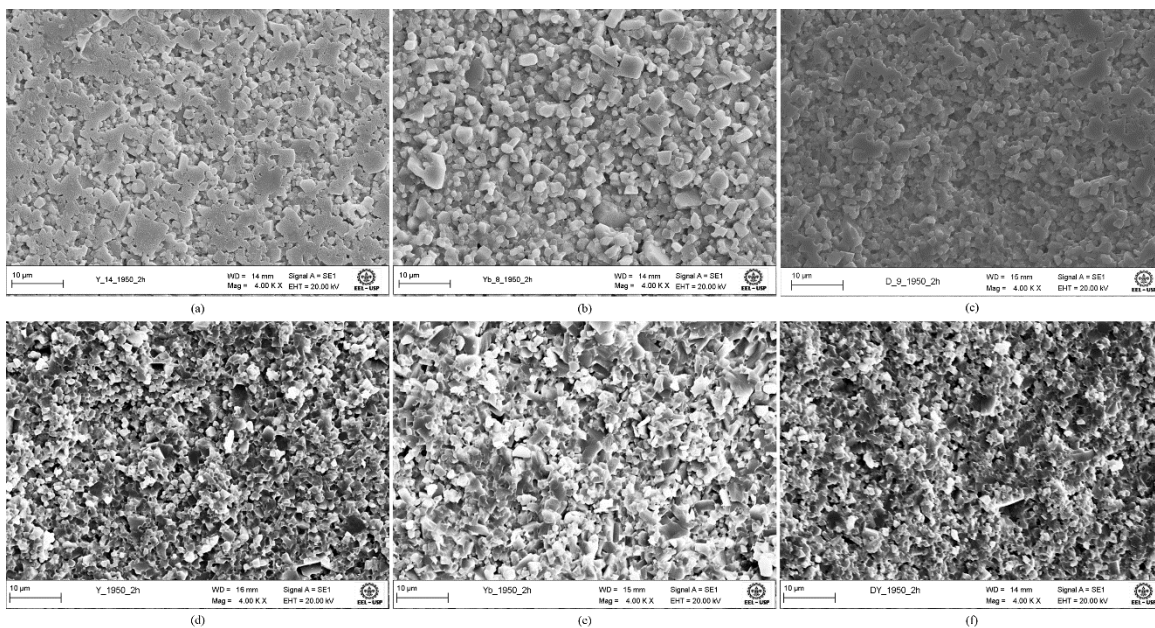


Figure 2. Secondary electron SEM images of the samples: (a, d) ALY; (b, e) ALYB; and (c, f) ALD, with (a, b, c) corresponding to the polished surfaces etched with sodium tetraborate, and (d, e, f) to the fracture surfaces.

4. Conclusions

An analysis of the results showed in Table 4, using the three different additives, it can be concluded that all the oxides can be used to produce the liquid phase sintered SiC ceramics.

The values of modulus of rupture, hardness and fracture toughness of SiC ceramics doped with mixtures of $\text{Al}_2\text{O}_3 + \text{Yb}_2\text{O}_3$ and $\text{Al}_2\text{O}_3 + \text{Dy}_2\text{O}_3$ are quite similar to those presented by $\text{Al}_2\text{O}_3 + \text{Y}_2\text{O}_3$, which are already well known in the literature.

The values found for SiC doped with $\text{Al}_2\text{O}_3 + \text{Y}_2\text{O}_3$ are comparable to those reported in the literature for liquid phase sintering without pressure.

References

1. Negita K. Effective sintering aids for silicon carbide ceramics: reactivities of silicon carbide with various additives. *Journal of the American Ceramic Society*. 1986; 69(12):C-308-310. <http://dx.doi.org/10.1111/j.1151-2916.1986.tb07398.x>.
2. Noviyanto A and Yoon D-H. Metal oxide additives for the sintering of silicon carbide: reactivity and densification. *Current Applied Physics*. 2013; 13(1):287-292. <http://dx.doi.org/10.1016/j.cap.2012.07.027>.
3. Noviyanto A and Yoon D-H. Rare-earth oxide additives for the sintering of silicon carbide. *Diamond and Related Materials*. 2013; 38: 124-130. <http://dx.doi.org/10.1016/j.diamond.2013.07.003>.
4. Biswas K, Rixecker G and Aldinger F. Gas pressure sintering of SiC sintered with rare-earth-(III)-oxides and their mechanical properties. *Ceramics International*. 2005; 31(5):703-711. <http://dx.doi.org/10.1016/j.ceramint.2004.06.027>.
5. Taguchi SP, Ribeiro S, Balestra RM and Rodrigues JD Jr. Infiltration of $\text{Al}_2\text{O}_3/\text{Y}_2\text{O}_3$ and $\text{AlN}/\text{Y}_2\text{O}_3$ mixes into SiC performs. *Materials Science and Engineering A*. 2007; 454-455:24-29. <http://dx.doi.org/10.1016/j.msea.2006.10.083>.
6. Ribeiro S, Taguchi SP, Motta FV and Balestra RM. The wettability of SiC ceramics by molten $\text{E}_2\text{O}_3(\text{ss})/\text{AlN}$ ($\text{E}_2\text{O}_3(\text{ss})$ = solid solution of rare earth oxides). *Ceramics International*. 2007; 33(4):527-530. <http://dx.doi.org/10.1016/j.ceramint.2005.10.026>.
7. Taguchi SP, Motta FV, Balestra RM and Ribeiro S. Wetting behaviour of SiC ceramics: Part II – $\text{Y}_2\text{O}_3/\text{Al}_2\text{O}_3$ and $\text{Sm}_2\text{O}_3/\text{Al}_2\text{O}_3$. *Materials Letters*. 2004; 58(22-23):2810-2814. <http://dx.doi.org/10.1016/j.matlet.2004.05.004>.
8. Motta FV, Balestra RM, Ribeiro S and Taguchi SP. Wetting behaviour of SiC ceramics: Part I – $\text{E}_2\text{O}_3/\text{Al}_2\text{O}_3$ additive system. *Materials Letters*. 2004; 58(22-23):2805-2809. <http://dx.doi.org/10.1016/j.matlet.2004.05.005>.

9. Strecker K, Ribeiro S and Hoffmann MJ. Fracture toughness measurements of LPS-SiC: a comparison of the indentation technique and the SEVNB method. *Materials Research*. 2005; 8(2):121-124. <http://dx.doi.org/10.1590/S1516-14392005000200004>.
10. Strecker K, Ribeiro S, Camargo D, Silva R, Vieira J and Oliveira F. Liquid phase sintering of silicon carbide with AlN/Y2O3, Al2O3/Y2O3 and SiO2/Y2O3 additions. *Materials Research*. 1999; 2(4):249-254. <http://dx.doi.org/10.1590/S1516-14391999000400003>.
11. Strecker K, Ribeiro S, Oberacker R and Hoffmann MJ. Influence of microstructural variation on fracture toughness of LPS-SiC ceramics. *International Journal of Refractory Metals & Hard Materials*. 2004; 22(4-5):169-175. <http://dx.doi.org/10.1016/j.ijrmhm.2004.05.001>.
12. Magnani G, Antolini F, Beaulardi L, Burrese E, Coglitore A and Mingazzini C. Sintering, high temperature strength and oxidation resistance of liquid-phase-pressureless-sintered SiC-AlN ceramics with addition of rare-earth oxides. *Journal of the European Ceramic Society*. 2009; 29(11):2411-2417. <http://dx.doi.org/10.1016/j.jeurceramsoc.2008.12.020>.
13. Klyucharev DS, Volkova NM and Comyn MF. The problem associated with using non-conventional rare-earth minerals. *Journal of Geochemical Exploration*. 2013; 133:138-148. <http://dx.doi.org/10.1016/j.gexplo.2013.03.006>.
14. Suzuki K and Sasaki M. Microstructure and mechanical properties of liquid-phase-sintered SiC with AlN and Y2O3 additions. *Ceramics International*. 2005; 31(5):749-755. <http://dx.doi.org/10.1016/j.ceramint.2004.08.014>.
15. da Silva JA, Moreschi BM, Garcia GCR and Ribeiro S. Wettability of silicon carbide ceramic by Al2O3/Dy2O3 and Al2O3/Yb2O3 systems. *Journal of Rare Earths*. 2013; 31(6):634-638. [http://dx.doi.org/10.1016/S1002-0721\(12\)60333-0](http://dx.doi.org/10.1016/S1002-0721(12)60333-0).